PHOTOCONVERSION FROM THE LIGHT-ADAPTED TO THE DARK-ADAPTED STATE OF BACTERIORHODOPSIN

T. KOUYAMA, R. A. BOGOMOLNI, AND W. STOECKENIUS
Cardiovascular Research Institute and Department of Biochemistry and Biophysics, University of California, San Francisco, San Francisco, California 94143

ABSTRACT Dark and light adaptation of bacteriorhodopsin in purple membrane multilayers at <100% relative humidity differs from that seen in suspensions. Equilibrium between the two bacteriorhodopsin isomers (bR^{cis}_{550} and bR^{trans}_{570}) in the light-adapted state becomes dependent on the wavelength of actinic light. Excitation at the red edge of the visible absorption band causes dark adaptation in a light-adapted sample. Using polarized actinic and measuring light, we show that acceleration of the dark adaptation through heating by actinic light cannot explain this observation. A light-driven bR^{trans}_{570} to bR^{cis}_{550} reaction that competes with the well-known 13 *cis*-to-all-*trans* light adaptation reaction must exist under our experimental conditions. *Trans*-to-*cis* conversion is a one-photon process distinct from the two photon process observed by others in purple membrane suspensions (Sperling, W., C. N. Rafferty, K. D. Kohl, and N. A. Dencher, 1978, *FEBS (Fed. Eur. Biochem. Soc.) Lett.* 97:129–132). Its quantum efficiency increases monotonously on reducing the hydration level, and is paralleled by an increase in the lifetime of the M_{410} intermediate of the *trans* photocycle. We suggest that at this point a branch leads from the all-*trans* into the 13-*cis* photocycle. It is probably the same reaction that causes the reduced light adaptation in monomeric bacteriorhodopsin (Casadio, R., H. Gutowitz, P. Mowery, M. Taylor, and W. Stoeckenius, 1980, *Biochim. Biophys. Acta.* 590:13–23; Casadio, R., and W. Stoeckenius, 1980, *Biochemistry.* 19:3374–3381).

INTRODUCTION

Bacteriorhodopsin (bR), the light-driven proton pump of halobacteria, exists in two interconvertible forms containing 13-*cis* and all-*trans* retinal isomers in their chromophores (1–4). The *cis* chromophore (bR^{cis}_{550}) has an absorption maximum at 548 nm, the *trans* chromophore (bR^{trans}_{570}) at 568 nm, and it has a 20% higher extinction coefficient. Dark-adapted bR in intact bacteria or in purple membrane (pm) suspensions absorbs maximally at 558 nm because an equilibrium is slowly established in the dark consisting of an equimolar mixture of the isomers (5, 6, 7, 8). In the light, each bR isomer undergoes distinct cyclic photoreactions. During the bR^{trans}_{570} photocycle a transient deprotonation of the Schiff base and isomerization around the C13, 14 double bond of the retinal take place (8–10) and four intermediates, K_{590}, L_{550}, M_{410}, and O_{640}, with lifetimes in the micro- and millisecond range have been characterized (the subscripts indicate the maxima of the visible absorption bands) (11, 12). Much less is known about the bR^{cis}_{550} photocycle, for which three intermediates, ^{x}C, ^{y}C, and ^{610}C, have been postulated. A branching point at ^{y}C is supposed to lead to bR^{trans}_{570} (13). At moderate light intensities, where the probability of photoexciting the thermal intermediates is low, the branching pathway from the 13-*cis* to the all-*trans* photocycle causes bR^{trans}_{570} to accumulate rapidly and a complete absence of bR^{cis}_{550} in the fully light-adapted pm has been generally assumed (1, 2, 6, 14–17).

The present work was originally undertaken to establish experimental conditions that excite the *trans* photocycle most efficiently in the optically dense pm films, which are used in x-ray and neutron diffraction studies, infrared spectroscopy, and measurement of charge shifts during the photoreaction cycle (18–21). Using excitation at the red edge of the visible absorption band to improve the penetration depth of the actinic beam we observed, however, that the red light caused dark adaptation of the pm film. This not only is of obvious practical importance, it also extends our earlier observation that suggested a thermal backreaction from intermediate(s) of the *trans* to the *cis* photoreaction cycle (1, 16) and we report here an investigation of this phenonemon.

MATERIALS AND METHODS

Purple membrane fragments were isolated from *Halobacterium halobium* (JW3) according to the established procedure (22). Optically clear pm films with no visible cracks even at low relative humidities with optical densities between 0.2 and 4.0 were prepared by an electrophoresis method (23). Briefly, an aqueous suspension of the pm fragments (~20 mg/ml; pH = 6–7) was sandwiched between In_2O_3-coated glass (Optical Coating Laboratory, Inc., Santa Rosa, CA) and Ag-coated glass, which served as the positive and negative electrodes, respectively. A direct current voltage of 1.7–2.8 V was applied between the two electrodes (separated by 0.1–1.0 mm) for 10–30 min and the membrane precipitated onto the

Correspondence should be addressed to Dr. R. A. Bogomolni.

transparent In_2O_3 electrode. The electrode with the film of stacked pm was dipped in a buffer solution (~0.1 M Tris-HCl; pH = 8) followed by distilled water and then dried at room humidity. For spectroscopic measurements the preparation was placed in a closed cuvette and the hydration level controlled with a small amount of the appropriate saturated salt solution (24).

A spectrophotometer capable of measuring absorption spectra of optically thick samples in the presence of actinic light was designed and built in our laboratory. A block diagram of the apparatus is shown in Fig. 1. An actinic light beam from a 300-W tungsten lamp or 500-W Xe lamp (L_a in Fig. 1) was passed through a series of optical filters, converted into a train of light pulses with a duration of 8 ms by a chopper rotating at 30 Hz, and then focused onto a sample holder. Light from another lamp (L_m 75 - W tungsten) was passed through a double monochromator (Cary 14; Varian Associates, Palo Alto, CA) and served as the measuring beam. When the actinic light was blocked the measuring beam was reflected, by a mirror on the chopper, into a photomultiplier tube (EMI9659QA; EMI, Inc., Clinton, CT). The output of the photomultiplier was sent to a logarithmic amplifier (755P; Analog Devices, Inc., Norwood, MA) and then to a sample-and-hold amplifier in which timing of the sampling mode was selected by logic pulses from a monitor of the chopper. The output of the second amplifier, the voltage of which is proportional to the logarithm of the peak value of the photocurrent, was digitized with an analog-to-digital converter and stored in a computer memory (1074; Nicolet Instrument Corp., Madison, WI). For scanning spectra, logic pulses from a wavelength monitor on the monochromator were used for memory address advance. The time needed to scan the wavelength from 330 to 740 nm was ~40 s. Experiments were carried on at 10°C unless otherwise stated.

RESULTS

Equilibrium between bR_{570}^{trans} and bR_{550}^{cis} in a Light-Adapted Purple Membrane Film

We found that equilibrium between the two bR isomers in light-adapted pm films depends on the wavelength of actinic light used and on the hydration of the sample. Although other physical parameters such as temperature, pH, and thickness of the sample also affect dark and light adaptation, we shall focus on the effects of these two parameters. Fig. 2 shows absorption changes at 590 nm (the maximum in the difference spectrum for dark and light-adapted bR) when a thermally fully dark-adapted film at 75% relative humidity is illuminated. Red light (615–660 nm; 2.2 mW/cm^2) causes a rapid decrease in absorbance due to accumulation of long-lived photointermediates (mainly, M_{412}) followed by a slow increase due to light adaptation. After 30 min a photostationary state is attained. When the red light is turned off, a fast increase in absorbance due to recovery of bR_{570}^{trans} and/or bR_{550}^{cis} from their photoproducts is followed by a slow decrease due to dark adaptation. When this procedure is repeated with a yellow light beam (510–660 nm; 7 mW/cm^2), the photostationary state has a lower absorbance because more pigment is cycling. The absorbance after the yellow illumination returns to a level higher than the one observed after illumination with red light. After reillumination with red light, the absorbance returns to the same level as observed after the first red light illumination.

The absorption spectra observed after light adaptation

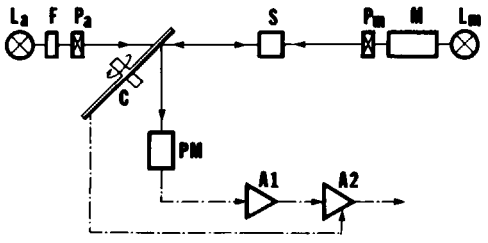

FIGURE 1 A schematic diagram of the spectrophotometer. L_a and L_m, light sources for actinic and measuring beams; *M*, double monochromator; *F*, optical filters; P_a and P_m, polarizers; *S*, sample holder; *C*, chopper with mirror; *PM*, photomultiplier tube; *A1*, logarithmic amplifier; *A2*, sample-and-hold amplifier.

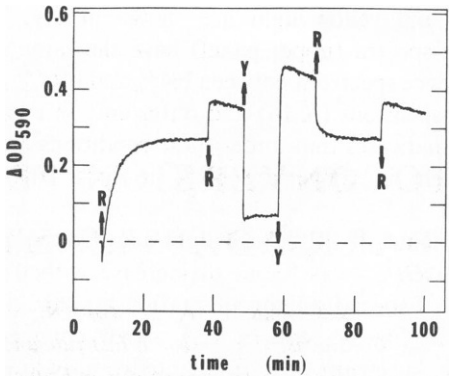

FIGURE 2 Absorption change at 590 nm when a dark-adapted pm film at 75% relative humidity is illuminated with red light (2 mW; 615–660 nm) and with yellow light (7 mW; 510–660 nm). The upward and downward arrows represent turn-on and turn-off of red (*R*) or yellow (*Y*) light, respectively. Absorbance at 590 nm in the dark-adapted state was 3.3 OD.

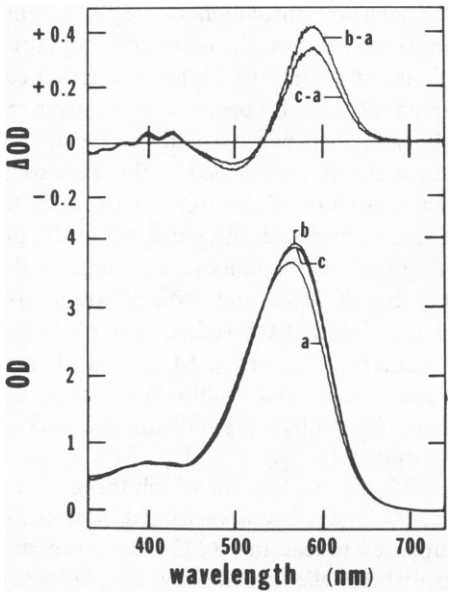

FIGURE 3 Absorption spectra of a pm film at 75% relative humidity in the dark-adapted state (*a*) and in light-adapted states (*b* and *c*). Curves *b* and *c* were recorded a few minutes after turning off the yellow light and the red light, respectively (see Fig. 2). The difference spectra between the dark-adapted and light-adapted states are shown in the *upper* panel.

with red and yellow light are shown in Fig. 3. Their difference spectra (upper panel) have the same shape as the difference spectrum between bR^{cis}_{550} and bR^{trans}_{570} observed for pm suspensions (6, 16) and differ only in extent. This therefore indicates that under these conditions red light is less efficient in converting bR^{cis}_{550} to br^{trans}_{570} than yellow light.

The amount of bR^{cis}_{550} in a light-adapted sample measured as ΔOD_{590} was found to increase with decreasing hydration. Especially light adaptation by red light (open symbols in Fig. 4) caused very small changes in the absorption spectrum of dark-adapted pm at low relative humidities. The decreased absorption change cannot be explained by a shift of the dark equilibrium toward bR^{trans}_{570} because the position of the absorption peak (at 560 nm) of the dark-adapted sample did not change significantly with decreasing relative humidity, except at extremely low relative humidity (Fig. 5), whereas the absorption peak of the light-adapted sample shifted from 570 to 560 nm when the relative humidity was lowered from 98 to 13%.

The Rate Constants of Dark and Light Adaptation

The rate constant of dark adaptation is nearly independent of the hydration level. The absorption change at 590 nm for the first 20–30 min after turning off the yellow beam decreased almost linearly with time. From the slope of this absorption decrease we estimated the time, $t_{1/10}$, during which dark adaptation increases by one-tenth of the full dark adaptation. In Fig. 6 *a*, the time constant $t_{1/10}$ is plotted as a function of relative humidity.

The rate constant of light adaptation was estimated from the rate of absorbance increase upon illumination of a dark-adapted sample (Fig. 2). When the actinic light is not very intense, the amount of long-lived intermediate(s) accumulating in the *trans* or *cis* photocycle is small and roughly proportional to the concentration of bR^{trans}_{570} and bR^{cis}_{550}. The absorbance at 590 nm in the presence of the actinic light is then linearly related to the concentrations of bR^{trans}_{570} and bR^{cis}_{550} in the sample. Except during the initial phase of the illumination when the amounts of photointermediates rapidly increase, the absorption change $A(t)$ substantially represents the change in the equilibrium between the two bR isomers. From the absorption kinetics recorded during light adaptation with red light, we calculated a halftime $t_{1/2}$ of light adaptation. In Fig. 6 *b*, the time constant $t_{1/2}$ is plotted as a function of relative

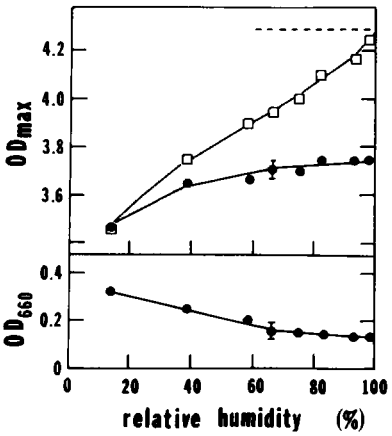

FIGURE 5 Absorbances at the absorption peak (*upper*) and at 660 nm (*lower*) for dark-adapted (closed circles) and the light-adapted (in yellow light; open squares) pm films are plotted as a function of relative humidity.

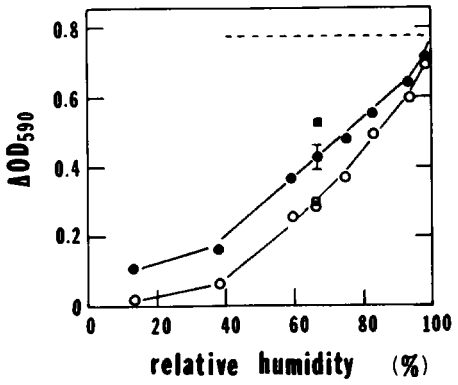

FIGURE 4 Absorption changes at 590 nm upon light adaptation of pm films as a function of relative humidity (pH 8). Closed and open circles represent the data obtained for yellow light (7 mW; 510–660 nm) and red light (2 mW; 615–660 nm), respectively. Closed and open squares show the corresponding absorption changes of a thinner film (OD_{560} – 0.25) after correction for thickness; the inner filter effect (or change in the spectral distribution) of actinic light is smaller for the thinner film. The dashed line represents the absorption change of a pm suspension of the same OD.

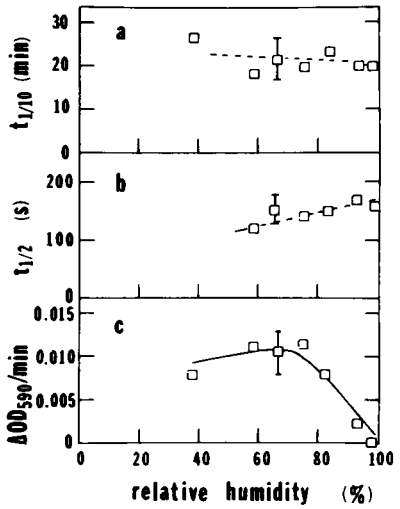

FIGURE 6 (*a*) Dependence of dark adaptation rate on relative humidity. $t_{1/10}$ is the time necessary to reach one-tenth of the full dark adaptation. (At low relative humidities, a very slow recovery of bR^{trans}_{570} or bR^{cis}_{550} from its photoproducts made it difficult to obtain accurate data.) (*b*) The halftime of light adaptation in red light (2 mW; 615–660 nm). (*c*) The initial rate of acceleration of dark adaptation by red light (1.7 mW; 630–660 nm); the experimental procedure is described in Fig. 7.

humidity. The rate constant of light adaptation increases upon dehydration. This change is opposite to the one expected if dehydration inhibited the light-driven *cis*-to-*trans* conversion. The acceleration of light adaptation cannot be accounted for by inner filter effects (i.e., the decreasing light intensity of the actinic beam in the sample caused by increasing amounts of bR_{570}^{trans}), because this effect is negligible at long excitation wavelengths (615–660 nm) and does not change significantly with relative humidity.

Acceleration of Dark Adaptation by Red Light

All of the results described above are explained satisfactorily by a light-driven conversion of bR_{570}^{trans} into bR_{550}^{cis}. This interpretation is further supported by the observation that dark adaptation is accelerated by red light. The absorption kinetics shown in Fig. 7 were recorded 2 min after a pm film at 66% relative humidity had been light-adapted with yellow light (510–660 nm; 7 mW/cm^2). The sample pulsed with red light during dark adaptation showed a 590-nm absorbance level, lower than that attained in the absence of illumination (Fig. 7 *a–c*).

The magnitude of the absorption decrease following the red-light pulse was independent of the time at which the pulse was applied; that is, red-light illumination 30 s and 11 min after turning off the yellow light beam caused essentially the same absorbance decrease. One might argue that an unknown photoproduct with significant absorption at 590 nm and a lifetime longer than 10 min accumulates in yellow light and is removed by red light. The difference absorption spectra shown in Fig. 3, however, clearly indicate that no photoproduct other than bR_{570}^{trans} is present after the yellow light has been turned off.

Because the rate of dark adaptation increases sharply with temperature, the question arises whether the acceleration of dark adaptation could be due to heating of the sample by the red light. We exclude this possibility, by using polarized actinic and measuring beams. The sample was first light-adapted with a nonpolarized yellow light (510–660 nm; 7 mW/cm^2) and then illuminated with a polarized red beam (630–660 nm; 0.5 mW/cm^2). The absorbance decrease was approximately three times larger with parallel polarization planes of the actinic and measuring beams were parallel than with perpendicular polarization (Fig. 7 *b*). If heating of the sample by the actinic light had caused the accelerated dark adaptation both polarization directions should give the same absorbance.

Acceleration of dark adaptation by red light depends on the level of hydration. In Fig. 6 *c*, the rate of the absorbance decrease during red illumination (630–660 nm; 1.8 mW/cm^2) is plotted as a function of relative humidity. At 98% relative humidity no absorbance decrease was detected. At 75% relative humidity it reached 0.011 OD per minute and decreased slightly at lower humidity.

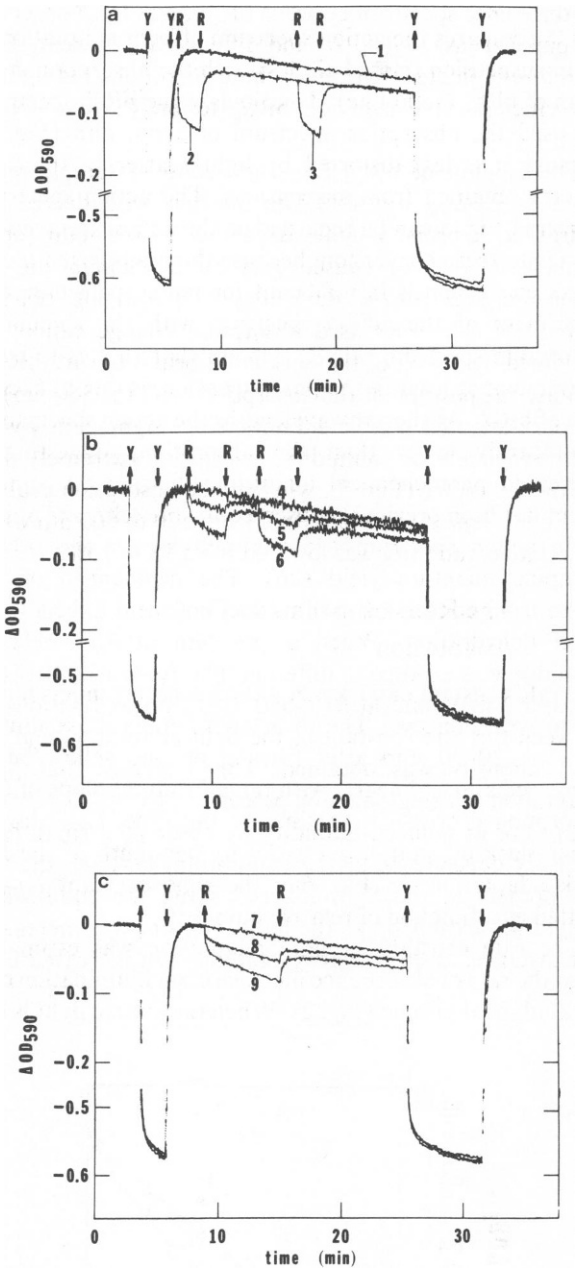

FIGURE 7 Acceleration of dark adaptation at 66% relative humidity by red light. The sample was first light-adapted in yellow light (7 mW; 510–660 nm) and the recording was started 2 min after turning off the yellow light. The large absorbance decreases at the beginning and at the end of the each curve are due to illumination with the yellow light. (*a*) Effects of red illumination. Curve *1* shows the absorbance changes of a sample kept in the dark. Curves *2* and *3* were obtained when a red light (630–660 nm) was turned on 30 s or 11 min after the yellow light. (*b*) Effect of polarized light. The measuring beam was vertically polarized. Curves *5* and *6* were obtained when the actinic beam (630–660 nm) was vertically and horizontally polarized, respectively. (*c*) Dependence of the accelerated dark adaptation on the light intensity. Curves *8* and *9* were obtained when the light intensity of the red actinic beam (635–645 nm) was 0.3 and 0.15 mW/cm^2, respectively.

Action Spectra and Light Intensity Dependence of Chromophore Conversion

Fig. 8 compares the action spectrum of light adaptation in a pm suspension (closed circles) with the absorption spectrum of bR_{550}^{cis} (solid line). To calculate the bR_{550}^{cis} spectrum we used the absorption spectrum of a pm film (Fig. 3) because it is less distorted by light scattering than the spectra obtained from suspensions. The action spectrum shown in Fig. 8 can be regarded as the action spectrum of the *cis*-to-*trans* conversion, because the light-driven *trans*-to-*cis* conversion is insignificant for pm suspensions. The agreement of the action spectrum with the calculated absorption spectrum of bR_{550}^{cis} shows that the *cis*-to-*trans* conversion, at least in the pm suspension, is due to excitation of bR_{550}^{cis}. At shorter wavelengths the action spectrum is significantly lower than the absorption suggesting a decreased photochemical quantum efficiency. A similar effect has been previously observed for the all-*trans* photocycle action spectrum (25) as well as for the proton pumping quantum yield (26). The mechanism of the *cis*-to-*trans* conversion in films does not seem to be altered upon dehydration. When a pm film at 75% relative humidity was exposed to different light intensities between 0.2 and 2 mW/cm^2 at 615–660 nm, a linear relationship between the rate constant of the light adaptation and the light intensity was obtained. This indicates that light adaptation is a single-photon process.

In films at reduced humidity we observed a small light intensity dependence of the equilibrium between the two bR isomers in the light-adapted state; the equilibrium shifted toward bR_{570}^{trans} as the light intensity was increased. For instance, at 66% relative humidity, an increase in the intensity of yellow light from 7 mW/cm^2 to 28 mW/cm^2 resulted in 0.5–1% increase in the amount of bR_{570}^{trans}. This dependence is the opposite of what one would expect if the bR_{570}^{trans} to bR_{550}^{cis} photoconversion were a two-photon process. We therefore conclude that the main pathway of the light-driven *trans*-to-*cis* conversion is also a single photon process. This conclusion is further supported by a linear increase in the rate of dark adaptation with red light intensity (Fig. 7 *c*). When the intensity of the red light (635–645 nm) was reduced from 0.3 to 0.15 mW/cm^2, the magnitude of the absorption drop observed after the illumination became approximately half.

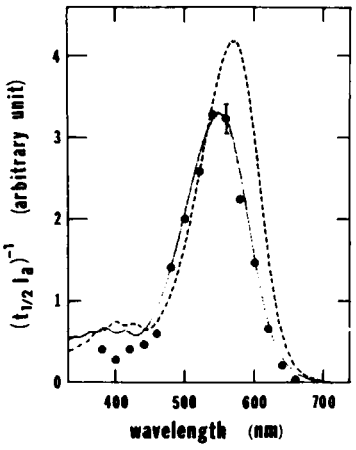

FIGURE 8 Closed circles represent the action spectrum for light adaptation in a pm suspension at pH 8 (OD_{560} = 0.08): $1/(t_{1/2} \cdot I_a)$, where $t_{1/2}$ is the halftime of light adaptation and I_a the actinic light intensity (quanta per seconds). Absorption spectra of bR_{550}^{cis} (solid line) and bR_{570}^{trans} (broken line) were calculated from the absorption spectra *a* and *b* in Fig. 3. In this calculation, we assumed that the dark-adapted sample contains an equimolar mixture of bR_{550}^{cis} and bR_{570}^{trans}; the equilibrium in the light-adapted state was estimated using the data shown in Fig. 4.

DISCUSSION

Absorption spectroscopy of dried pm multilayers at very low relative humidity has shown large blue shifts of the bR absorption band (27). We are concerned here only with preparations at relative humidities >13% where these blue shifted species are undetectable. The present study demonstrates a light-driven conversion of bR_{570}^{trans} into bR_{550}^{cis} in partially dried pm films. A reduction in the extent of light adaptation similar to the one described here also occurs in bR monomers solubilized with Triton X-100 (2) and monomeric bR in lipid vesicles (16, 28); it has been ascribed to a backreation from bR_{570}^{trans} photocycle intermediate(s) to the bR_{550}^{cis} cycle (2). A superficially also similar "dark adaptation by light" has been reported for aqueous suspensions of pm (1). However, the actinic light used in those experiments had an $\sim 10^6$ times higher intensity and the effect is apparently due to a two-photon mechanism, whereas the *trans*-to-*cis* conversion in dried samples described here is a single photon process. We have not checked whether a similar two-photon effect also occurs in partially dried preparations.

The presence of bR_{550}^{cis} in light-adapted pm films at reduced humidity was first investigated by Korenstein and Hess and explained as due to an inhibition of light-driven *cis*-to-*trans* conversion (29). This explanation is inconsistent with our observation that the rate of light adaptation increases at lower relative humidity (Fig. 6 *b*). The apparent rate of light adaptation

$$bR_{550}^{cis} \underset{k_-}{\overset{k_+}{\rightleftharpoons}} bR_{570}^{trans}$$

is determined by the sum of the conversion rates in the two directions: $k_{ap} = k^+ + k^-$ and the amount of bR_{550}^{cis} in the light-adapted state is proportional to $k^-/(k^+ + k^-)$. The monotonous increase in bR_{550}^{cis} with the decreasing relative humidity (Fig. 4) is consistent with an increase in the rate k^- with little change in k^+. This suggestion is supported by the observed initial rates of dark adaptation by red light (Fig. 6 *c*). These initial rates should be proportional to $[A(\infty) - A(0)](k^+ + k^-)$. Where $A(\infty)$ and $A(0)$ are the absorbances of the samples fully light-adapted with yellow

and red light, respectively. When this rate is calculated from the data shown in Figs. 4 and 6 *b* it fits the experimental points (Fig. 6 *c*).

If the photocycle in partially dehydrated films proceeds via the same intermediates as in pm suspensions (30), a branching point leading into the bR^{cis}_{550} cycle must exist. The latest likely branching point is at M_{410} because it is the last intermediate with a 13-*cis* conformation (10) and a rapid thermal isomerization around the C13-14 double bond is unlikely (31). In order to decide whether the branching occurs before or after formation of M_{410}, we subtracted from the absorption spectra of the photostationary state in yellow light the spectrum recorded a few minutes after the actinic light had been turned off (Fig. 9). The difference spectra show a positive peak at 410 ± 2 nm and a zero-crossing point at 457 ± 3 nm, only spectra of samples below 58% relative humidity show a weak positive peak near 660 nm. These features are essentially the same found in difference spectra of suspensions containing mainly bR^{trans}_{570} and its long-lived photoproduct, M_{410} (32, 33). However, the position of the large negative peak shifts from 570 nm to 569 nm, 565 nm and 556 nm in films at 93%, 75%, 58%, and 13% relative humidity. This shift would be expected if branching of M_{410} into the *cis* photocycle occurs and increases with decreasing hydration. Let f be the probability that M_{410} decays to bR^{cis}_{550}. Then the difference spectrum $\Delta A(\lambda)$ is approximated by the following equation:

$$\Delta A(\lambda) = [\epsilon^{M}(\lambda) - (1 - f)\epsilon^{t}(\lambda) - f\epsilon^{c}(\lambda)]\,[M]_{on},$$

where ϵ^{M}, ϵ^{t}, and ϵ^{c} represent the absorption coefficients of M_{410}, bR^{trans}_{570}, and bR^{cis}_{550}, respectively, and $[M]_{on}$ the amount of M_{410} in a photostationary state. This equation shows how an increase in the value of f causes a blue shift of the negative peak in the difference spectrum. We have assumed that in the photostationary state M_{410} is the only intermediate accumulated in significant amounts. This approximation is valid at least at or above 58% relative humidity because the difference spectrum $\Delta A(\lambda)$ for 58% relative humidity divided by a constant and then subtracted from the $\Delta A(\lambda)$ for 93% relative humidity yields a spectrum with the same profile as the light dark adaptation difference spectrum $\epsilon^{t}(\lambda) - \epsilon^{c}(\lambda)$.

Another argument for branching at M_{410} into the bR^{cis}_{550} cycle is derived from the equilibria between the two bR isomers after exposure of pm films to high light intensities. If branching occurs before M_{410}, the equilibrium between the two bR isomers after turning off the actinic light would shift toward bR^{trans}_{570} with increasing light intensity in proportion to the increase in M_{410} generated. The experimentally observed shift was far smaller than expected and may be due to light absorption by an earlier intermediate, e.g., L_{550} (34). Therefore a fraction of M_{410} must decay to bR^{cis}_{550}.

The lifetime of M_{410} correlates with the efficiency of the *trans*-to-*cis* photoconversion. In Fig. 10 *a*, the absorbance

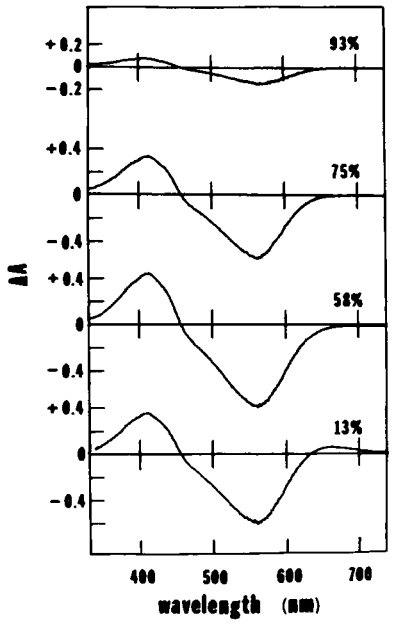

FIGURE 9 Difference spectra for photostationary states at different relative humidities. The spectra recorded a few minutes after turning off the actinic light have been subtracted from the spectra obtained in the presence of yellow light (7 mW; 510–660 nm).

change at 590 nm immediately after the red illumination (Fig. 2) is plotted as a function of relative humidity. For the relatively low light intensity used, this quantity (divided by the bR^{trans}_{570} concentration) should be approximately proportional to the product of the M_{410} decay time and the quantum efficiency of its formation. Since the latter does not vary with the hydration level (29), Fig. 10 *a* shows that the decay time of M_{410} increases monotonously with decreasing hydration. Similar to the dependence

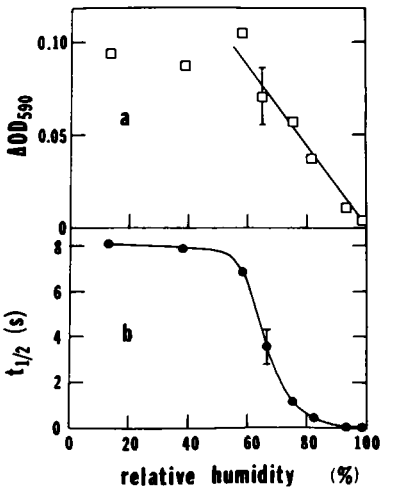

FIGURE 10 Plotted as a function of relative humidity are: (*a*) the amplitude of the absorption recovery at 590 nm immediately after turning off the red light and (*b*) the halftime of the absorption recovery at 410 nm (or 590 nm) after turning off the actinic (yellow) light; i.e., the halftime of M_{410} decay.

deduced above for the rate k_-, this correlation then suggests that the M_{410} to bR_{570}^{trans} process is strongly inhibited by reducing the hydration level, while the M_{410} to bR_{550}^{cis} process is affected less or not at all, thus increasing the efficiency of the *trans*-to-*cis* cycle transition.

We investigated the decay of M_{410} by measuring absorbance recovery at 590 nm or decrease at 410 nm in the dark (Fig. 2). The kinetics required three exponential components for a satisfactory fit, as already reported by Korenstein and Hess (30). In Fig. 10 *b*, the halftime of the absorbance recovery is plotted as a function of relative humidity. This time is not necessarily proportional to the average lifetime, because the longer-lived fraction(s) of M_{410} will accumulate proportionally in the photostationary state and there is no linear correlation between it and the reduction in light adaptation shown in Fig. 10 *a*. Presumably contribution by the fraction of M_{410} with an extremely long lifetime (on the order of minutes) becomes more significant at lower relative humidity. Because the kinetics did not change much with light intensity the long-lived component is not due to cooperativity between neighboring bR molecules. A more probable explanation for the long lifetime is that some of the proton uptake or transfer processes involved in the pathway from M_{410} to bR_{570}^{trans} or bR_{550}^{cis} are inhibited at reduced hydration.

We are grateful to Drs. R. H. Lozier and W. Sperling for extensive discussion.

This work was supported by a National Institues of Health Program Project grant GM-27057 and National Aeronautics and Space Administration grant NSG-7151.

Received for publication 14 May 1984 and in final form 22 January 1985.

REFERENCES

1. Sperling, W., C. N. Rafferty, K. D. Kohl, and N. A. Dencher. 1978. Isomeric composition of bacteriorhodopsin under different environmental light conditions. *FEBS (Fed. Eur. Biochem. Soc.) Lett.* 97:129–132.
2. Casadio, R., H. Gutowitz, P. Mowery, M. Taylor, and W. Stoeckenius. 1980. Light-dark adaptation of bacteriorhodopsin in Triton-treated purple membrane. *Biochim. Biophys. Acta.* 590:13–23.
3. Oesterhelt, D., and W. Stoeckenius. 1971. Rhodopsin-like protein from the purple membrane of *Halobacterium halobium*. *Nature New Biol.* 233:149–152.
4. Oesterhelt, D., M. Meentzen, and L. Schuhmann. 1973. Reversible dissociation of the purple complex in bacteriorhodopsin and identification of 13 *cis* and all-*trans* retinal as its chromophores. *Eur. J. Biochem.* 40:453–463.
5. Schreckenbach, T., and D. Oesterhelt. 1977. Photochemical and chemical studies on the chromophore of bacteriorhodopsin. *Fed. Proc.* 36:1810–1814.
6. Sperling, W., P. Carl, C. N. Rafferty, and N. A. Dencher. 1977. Photochemistry and dark equilibrium or retinal isomers and bacteriorhodopsin isomers. *Biophys. Struct. Mech.* 3:79–94.
7. Maeda, A., T. Iwasa, and T. Yoshizawa. 1977. Isomeric composition of retinal chromophore in dark-adapted bacteriorhodopsin. *J. Biochem. (Tokyo).* 82:1599–1604.
8. Pettei, M. J., A. P. Yudd, K. Nakanishi, R. Henselman, and W. Stoeckenius. 1977. Identification of retinal isomers isolated from bacteriorhodopsin. *Biochemistry.* 16:1955–1959.
9. Lewis, A., J. Spoonhower, R. A. Bogomolni, R. H. Lozier, and W. Stoeckenius. 1974. Tunable laser resonance Raman spectroscopy of bacteriorhodopsin. *Proc. Natl. Acad. Sci. USA.* 71:4462–4466.
10. Smith, S., J. A. Pardoen, J. Lugtenburg, B. Curry, and R. Mathies. 1983. Chromophore structure in bacteriorhodopsin's O_{640} photointermediate. *Biochemistry.* 22:6141–6148.
11. Lozier, R. H., R. A. Bogomolni, and W. Stoeckenius. 1975. Bacteriorhodopsin: A light-driven proton pump in *Halobacterium halobium*. *Biophys. J.* 15:955–962.
12. Dencher, N., and M. Wilms. 1975. Flash photometric experiments on the photochemical cycle of bacteriorhodopsin. *Biophys. Struct. Mech.* 1:259–271.
13. Sperling, W., C. N. Rafferty, K. D. Kohl, and N. A. Dencher. 1978. Effect of light on the isomer composition of bacteriorhodopsin in the purple membrane of *Halobacterium halobium*. *In* Energetics and Structure of Halophilic Microorganisms. S. R. Caplan and M. Ginzburg, editors. Elsevier/North Holland, Amsterdam. 321–330.
14. Kalisky, O., C. R. Goldschmidt, and M. Ottolenghi. 1977. On the photocycle and light adaptation of dark-adapted bacteriorhodopsin. *Biophys. J.* 19:185–189.
15. Lozier, R. H., W. Niederberger, M. Ottolenghi, G. Sivorinovsky, and W. Stoeckenius. 1978. On the photocycles of light- and dark-adapted bacteriorhodopsin. *In* Energetics and Structure of Halophilic Microorganisms. S. R. Caplan, and M. Ginzburg, editors. Elsevier/North-Holland Biomedical Press, New York. 123–141.
16. Casadio, R., and W. Stoeckenius. 1980. Effect of protein-protein interaction on light adaptation of bacteriorhodopsin. *Biochemistry.* 19:3374–3381.
17. Iwasa, T., F. Tokunaga, and T. Yoshizawa. 1981. Photochemical reaction of 13-*cis* bacteriorhodopsin studied by low temperature spectrophotometry. *Photochem. Photobiol.* 33:539–545.
18. Rothschild, K. J., M. Zagaeski, and W. A. Cantore. 1981. Conformational changes of bacteriorhodopsin detected by Fourier transform infrared difference spectroscopy. *Biochem. Biophys. Res. Commun.* 103:483–489.
19. Bagley, K., G. Dollinger, L. Eisenstein, A. K. Singh, and L. Zimanyi. 1982. Fourier transform infrared difference spectroscopy of bacteriorhodopsin and its photoproducts. *Proc. Natl. Acad. Sci. USA.* 79:4972–4976.
20. Varo, G., and L. Keszthelyi. 1983. Photoelectric signals from dried oriented purple membranes of *Halobacterium halobium*. *Biophys. J.* 43:47–51.
21. Stamatoff, J., R. H. Lozier, and S. Gruner. 1982. X-ray diffraction studies of light interactions with bacteriorhodopsin. *Methods Enzymol.* 88:282–286.
22. Oesterhelt, D., and W. Stoeckenius. 1974. Isolation of the cell membrane of *Halobacterium halobium* and its fractionation into red and purple membrane. *Methods Enzymol.* 31:667–678.
23. Varo, G. 1982. Dried oriented purple membrane samples. *Acta Biol. Acad. Sci. Hung.* 32:301–310.
24. Wexler, A., and S. Hasegawa. 1954. Relative humidity-temperature relationships of some saturated salt solutions in the temperature range 0 to 50°C. *J. Res. Natl. Bur. Stand.* 53:19–26.
25. Weber, H. J., and R. A. Bogomolni. 1981. P588, a second retinal-containing pigment in *Halobacterium halobium*. *Photochem. Photobiol.* 33:601–608.
26. Bogomolni, R. A., R. A. Baker, R. H. Lozier, and W. Stoeckenius. 1980. Action spectrum and quantum efficiency for proton pumping in *Halobacterium halobium*. *Biochemistry.* 19:2152–2159.
27. Lazarev, Y. A., and E. L. Terpugov. 1980. Effect of water on the structure of bacteriorhodopsin and photochemical processes in purple membranes. *Biochim. Biophys. Acta.* 590:324–338.
28. Dencher, N. A., K. -D. Kohl, and M. P. Heyn. 1983. Photochemical cycle and light-dark adaptation of monomeric and aggregated

bacteriorhodopsin in various lipid environments. *Biochemistry.* 22:1323–1334.

29. Korenstein, R., and B. Hess. 1977. Hydration effects on *cis trans* isomerization of bacteriorhodopsin. *FEBS (Fed. Eur. Biochem. Soc.) Lett.* 82:7–11.
30. Korenstein, R., and B. Hess. 1977. Hydration effects on the photocycle of bacteriorhodopsin in thin layers of purple membrane. *Nature (Lond.).* 270:184–186.
31. Orlandi, G., and K. Schulten. 1979. Coupling of stereochemistry and proton donor-acceptor properties of a Schiff base: A model of a light-driven proton pump. *Chem. Phys. Lett.* 64:370–374.
32. Oesterhelt, D., and B. Hess. 1973. Reversible photolysis of the purple complex in the purple membrane of *Halobacterium halobium.* *Eur. J. Biochem.* 37:316–326.
33. Kalisky, O., M. Ottolenghi, B. Honig, and R. Korenstein. 1981. Environmental effects on formation and photoreaction of M412 photoproduct of bacteriorhodopsin: Implications for the mechanism of proton pumping. *Biochemistry.* 20:649–655.
34. Hurley, J. B., B. Becher, and T. G. Ebrey. 1978. More evidence that light isomerises the chromophore of purple membrane protein. *Nature (Lond.).* 272:87–88.